

Triarylphosphonium BODIPY-Based [2]Rotaxanes Nanoparticles for Light-Driven Antibacterial Applications

Greta Sambucari, Corinne Coutant, Alessandro Di Michele, Gina Elena Giacomazzo, Pierrick Nun, Vincent Sol, Noe Renard, Tan-Sothea Ouk, Vincent Coeffard, Mariangela Di Donato**

Greta Sambucari, Mariangela Di Donato

LENS, via N. Carrara 1, 50019 Sesto Fiorentino (FI), Italy

Mariangela Di Donato CNR-ICCOM, via Madonna del Piano 10, 50019 Sesto Fiorentino (FI), Italy.

E-mail: didoanto@lens.unifi.it

Corinne Coutant, Pierrick Nun, Vincent Coeffard

CEISAM UMR CNRS 6230, Nantes Université, F-44000 Nantes, France.

E-mail: Vincent.Coeffard@univ-nantes.fr

Alessandro di Michele

Dipartimento di Fisica e Geologia, Università di Perugia, Via A. Pascoli , 06123 Perugia, Italy

Gina Elena Giacomazzo

Dipartimento di Chimica, Università di Firenze, via della Lastruccia 3-13, 50019 Sesto Fiorentino (FI), Italy

Vincent Sol, Noe Renard, Tan-Sothea Ouk

Université de Limoges, LABCiS UR22722, F-87000, Limoges, France

Abstract

Antimicrobial photodynamic therapy (aPDT) is a promising strategy to overcome issues related to antibiotic resistance. Here we describe the rationale for designing new photosensitizers based on the functionalization of bodipy dyes with triarylphosphonium rotaxanes and provide an in-depth characterization of their photophysical properties, applying different spectroscopic techniques, including ultrafast transient absorption spectroscopy. While the addition of halogen atoms to some of our structures provides them the ability to efficiently produce singlet oxygen in organic solvents, such property is suppressed in water, where all the investigated compounds aggregate into spherical nanoparticles. The latter, independently of the presence of bromine, demonstrate high photothermal conversion efficiency, and have been tested as photosensitizers in antibacterial photothermal therapy, highlighting the potential of self-assembled organic nanostructures based on bodipy dyes for developing new and versatile nanomaterials for photomedicine applications.

Keywords: antimicrobial photodynamic therapy, bodipy, rotaxanes, ultrafast spectroscopy, photothermal effect

1. Introduction

Antimicrobial resistance, mostly associated with the widespread use of broad-spectrum antibiotics, is a major challenge for public health, causing a rising number of serious infections and severely increasing mortality among patients.^[1] The past decades have indeed witnessed the emergence of multi-drug resistant bacteria and pathogens, accompanied by a dramatic growth of infections not treatable with conventional antibiotic therapies. A primary concern associated with the emergence of antimicrobial resistance relies on the fast rate of resistance acquisition, that bacteria develop either from prior generations as well as from other strains and species.^[2] The problem also extends to infections caused by fungi and parasites, urgently boosting the necessity to develop alternative treatments. To worsen this scenario, in recent times the development of new antibiotics has greatly decreased, because of economic and regulation problems,^[3] making the search for new approaches to treat this problem urgent and timely. Among others, photodynamic therapy, originally developed to treat several types of cancerous lesions, has recently raised an increasing interest as an alternative method of killing bacteria and fungi.^[4] Photodynamic therapy, also in its antimicrobial application (aPDT), uses light to activate a chemical species, termed photosensitizer (PS), which can efficiently undergo intersystem crossing (ISC) generating triplet species. The latter, can either directly react with oxygen, producing singlet oxygen (type II mechanism, or undergo electron transfer with different substrates, producing various reactive oxygen species (ROS), such as hydroxyl radicals or superoxide anions (type I mechanism), which are all cytotoxic compounds.^[5]

One of the main advantages of PDT relies on its ability to produce strong oxidant species, which can kill bacteria and microbes by damaging their vital structures as proteins, membranes and DNA, with very high spatio-temporal control, since it relies on a light triggering. Furthermore, this method has a very wide action spectrum and can be applied to the eradication of different strands of bacteria, fungi, protozoa and viruses, independently from their developed drug resistance.^[6]

Despite the great potential of PDT and aPDT, only a limited number of PSs are currently being approved for clinical use, mostly based on porphyrin derivatives.^[5c, 7] Given the great promises of these therapeutic methods in the last few years, a growing number of potential PS candidates have been synthesized and tested, in some cases with good perspectives for their *in vivo* application.^[8] The research focus is on identifying new compounds with optimal properties, such as high absorption coefficient, extended photostability, high ISC yield and possibly good

water solubility, which is required for acting in a biological environment. Furthermore, considering the possible damage that UV and blue light can produce to biological tissues, cells and DNA and the limited penetration depth of short wavelength radiation, an ideal PS should absorb in the red/near IR spectral region.

Bodipy chromophores have been the object of increasing interest, and have been often used as building blocks for the development of new PSs,^[9] because of their favorable physico-chemical properties, including high absorbance and fluorescence, great photostability, ease of synthesis and derivatization,^[10] which open up the possibility of modulating their spectral properties and red-shifting their absorption spectrum, by appending different functional group to the bodipy core.^[9a]

Here we present and characterize new [2]rotaxane-based bodipy (BDP) PSs (**Br**)-BDP2-3 for applications in aPDT, where the bodipy core bears a pendant benzo-crown ether, which can further be functionalized through a threading-followed-by-stoppering approach using two triarylphosphonium stoppers (Figure 1).^[11] Rotaxane-type photosensitizers have been proposed for PDT applications,^[12] but benzo-crown ether functionalized chromophores were generally designed to act as cation sensors,^[13] and such systems incorporated in bodipy-based supramolecular assemblies have never been applied in aPDT. To increase triplet formation, three of our derivatives (**Br**-BDP1; **Br**-BDP2 and **Br**-BDP3) were further functionalized with two bromine atoms, with the aim of increasing the ISC yield based on the heavy atom effect.^[14]

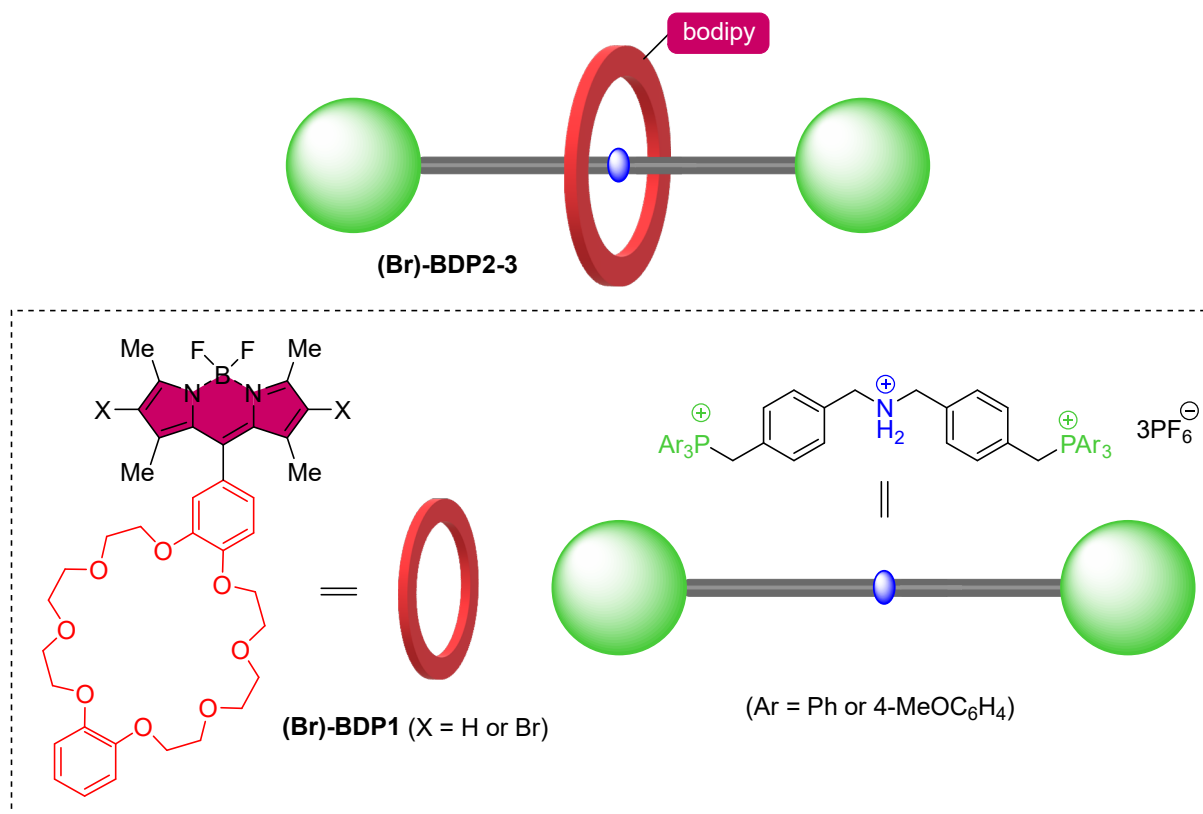


Figure 1. Supramolecular assemblies based on functionalized bodipy chromophores.

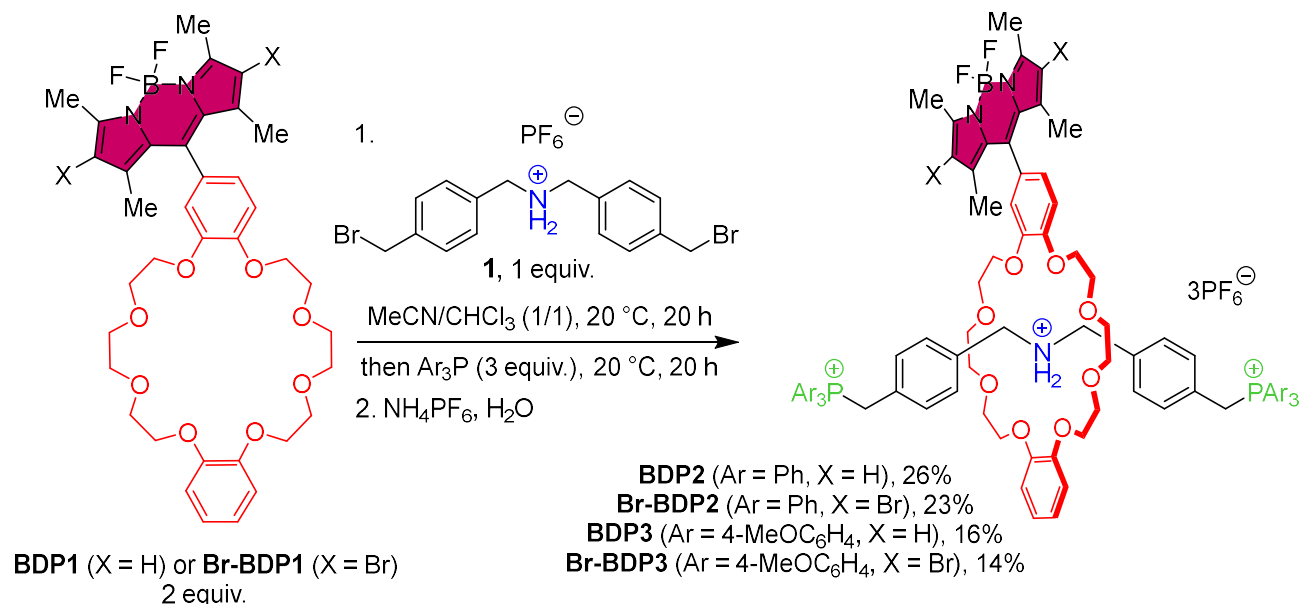
Besides the bodipy dye, the supramolecular assemblies are composed of two important structural motifs, which are the benzo-crown ether and the phosphoniums stoppers. The idea of exploiting crown ether functionalization came from the ability of ether-based macrocycles to form bodipy-based rotaxanes for applications in fluorescence imaging.^[15] In a recent work it has been found that such functionalization reduced triplet-triplet annihilation,^[16] increasing triplet lifetime, which is expected to translate in a higher PDT activity. It was also suggested that such compounds could undergo photoinduced charge transfer (CT) from the crown ether to the bodipy core, that we confirm by applying transient absorption spectroscopy. A crucial parameter in light-active antibacterial agents is their ability to selectively target bacteria. One common strategy relies on the electrostatic interactions of the photosensitizer with the bacteria cell wall.^[17] Given the negatively charged nature of the bacterial cell wall, a common approach is to introduce positively charged groups onto the BODIPY dye.^[18] While quaternary ammonium groups have been widely used in aPDT, examples of phosphonium-functionalized dyes exhibiting high affinity for the bacterial cell wall remain scarce in the literature.^[19] We surmised that the introduction of two phosphonium functional groups would enhance the interactions with the bacteria cell wall.

In the following, we present the synthesis and the complete photochemical characterization of six new PSs, involving the analysis of their photodynamic behavior using ultrafast transient absorption spectroscopy. Our compounds were initially designed to act as PSs in aPDT through ISC and singlet oxygen generation, which we confirm in the case of brominated species when dissolved in organic solvents. However, if solubilized in water all the investigated BDP-based molecules form aggregates, whose fluorescence yield and ISC ability are greatly reduced. Nevertheless, as their excited state lifetime becomes extremely short, the compounds resulted highly effective in producing heat once photoexcited. We thus evaluated their efficiency as photothermal agents, discovering that these systems, independently of the presence of bromine, have quite high photothermal efficiency, as demonstrated through their successful application in killing planktonic bacterial strains of Gram-positive (*Staphylococcus aureus*) and Gram-negative (*Escherichia coli*).

2. Results and discussion

2.1. Molecular design and Synthesis

The synthesis of the [2]rotaxanes **(Br)-BDP2-3** is illustrated in Scheme 1. The benzo-crown ether bodipy dyes **(Br)-BDP1** and the ammonium axle **1** were synthesized following reported procedures as described in Section 2 of the Supporting Information.



Scheme 1. Rotaxane synthesis through a threading-followed-by-stoppering approach.

The preparation of rotaxanes **(Br)-BDP2-3** is based on the formation of a pseudorotaxane supramolecular assembly between the functionalized dibenzylammonium cation **1** and the benzo-crown ether bodipy **(Br)-BDP1**, followed by nucleophilic substitutions of the bromo groups by triarylphosphines to install the bulky triarylphosphonium stoppers, according to the work of Stoddart.^[11] After counter anion exchange (NH₄PF₆, H₂O), **(Br)-BDP2-3** rotaxanes were isolated in yields ranging from 14% to 26%. The threading of the dibenzylammonium binding motif with the benzo-crown ether bodipy **(Br)-BDP1** to form the corresponding pseudorotaxane is a crucial step in preparing the targeted rotaxanes. Therefore, a careful screening of solvent conditions was carried out for a 1:1 mixture of **BDP1:1**, and association constants were determined by ¹H NMR due to the fact that free species and the pseudorotaxane are in slow exchange on NMR timescale (See Supporting Information for further details). The best value ($K_a = 988 \text{ L}\cdot\text{mol}^{-1}$) was obtained in CD₃CN/CDCl₃ (1:1). Further screening of **BDP1:1** ratio showed that the reaction of 1 equiv. of axle **1** with 2 equivalents of benzo-crown ether bodipy gives the best yield (26%). The introduction of bromine atoms on the bodipy framework did not influence the rotaxane yield, and the product **Br-BDP2** was obtained in 23% yield. Attempts to prepare the 2,6-diiodo-bodipy-derived rotaxane led to the removal of the iodine atoms during the substitution step with triphenylphosphine.^[20] The use of a bulkier

phosphine, (4-MeOC₆H₄)₃P, led to lower yields of rotaxanes and the products **BDP3** and **Br-BDP3** were isolated in 16% and 14% yields, respectively. Trialkylphosphines (*e.g.* tributylphosphine, tris(hydroxypropyl)phosphine) failed to react to form the desired rotaxanes.

2.2. Spectroscopic properties

We initially investigated the spectroscopic properties of our compounds in the polar organic solvent acetonitrile (ACN). The absorption spectra of the compounds, reported in Figure 2a), are typical for bodipy dyes, presenting an intense and sharp band respectively peaked at 498 nm and 522 nm respectively for non brominated and brominated molecules.

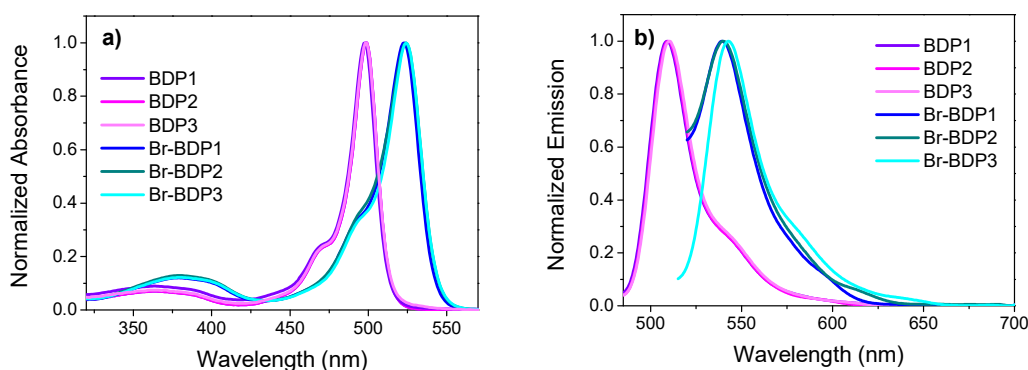


Figure 2: a) absorption and b) emission spectra of **BDP1-3** and **Br-BDP1-3** measured in acetonitrile at room temperature. Fluorescence has been recorded upon excitation at 480 nm and 510 nm respectively for non brominated and brominated molecules.

Emission bands appear as mirror images of the absorption spectra and present Stoke shifts of about 10-17 nm, respectively peaking at 509/510 nm and 539/540 nm for non brominated and brominated compounds. Molar absorption coefficients were estimated on the order of 10^4 ranging from $35\,000\text{ M}^{-1}\text{ cm}^{-1}$ to almost $80\,000\text{ M}^{-1}\text{ cm}^{-1}$. The fluorescence quantum yields of the compounds are all reduced as compared to a reference bodipy lacking of the appended crown ether. For non brominated compounds, decreased fluorescence yields could be ascribed to the possibility of photoinduced charge transfer between the appendant and the bodipy core. Indeed fluorescence quenching is higher for **BDP1**, lacking of positive charged species inside the ether ring, which partially compensate the electron donating ability of the crown oxygens. In the case of brominated compounds, the possibility of ISC further decreases the emission yield, nevertheless, the comparison with a reference brominated bodipy lacking of the appendant ether, indicates that a contribution of charge transfer is evident also in this case.

Triplet formation in the case of brominated compounds is confirmed by measuring their singlet oxygen quantum yield (ϕ_{Δ}), using Rose Bengal as a reference compound. Triplet formation appears more efficient for **Br-BDP2** and **Br-BDP3** as compared with **Br-BDP1**, possibly because of the reduced contribution of photoinduced charge transfer. The spectroscopic properties of the compounds are summarized in Table 1, where the properties of the reference compounds **BDP0** and **BrBDP0** (bodipy lacking of the crown ether, respectively without and with bromine) are also listed.

Table 1. Spectroscopic properties of the compounds in ACN

Compound	λ_{abs} [nm]	λ_{em} [nm]	ϵ [M ⁻¹ cm ⁻¹]	ϕ_{em}	ϕ_{Δ}^{a}
BDP1	498	509	49995	0.21± 0.02	//
BDP2	498	509	75121	0.50± 0.02	//
BDP3	499	510	66941	0.52± 0.02	//
Br-BDP1	522	539	76958	≤0.02	0.17 ± 0.02
Br-BDP2	522	539	63030	0.098±0.02	0.58 ± 0.03
Br-BDP3	523	540	70745	0.092±0.02	0.59 ± 0.03
BDP0	497	509	73432	0.74± 0.02	//
Br-BDP0	522	540	35070	0.36± 0.02	0.56 ± 0.03

^{a)}Measured by determining the oxygen phosphorescence and using Rose Bengal as a reference(ϕ_{Δ} =0.53)

We then sought to characterize the spectroscopic properties of the compounds in water. By increasing the water content in the ACN solutions (from 1:10 ACN:water ratio to 1:99 ACN:water ratio) the absorption band gradually broadens and red shifts, suggesting the formation of aggregates (see Figure S1), as often observed in the case of differently functionalized hydrophobic bodipys.^[21] The effect is particularly evident for **BDP1** and **Br-BDP1**, lacking of charged species inside the crown ether, as shown in Figure 3 a) and b), which report the absorption spectra of the compounds measured in a mixed 1:99 ACN:water solution.

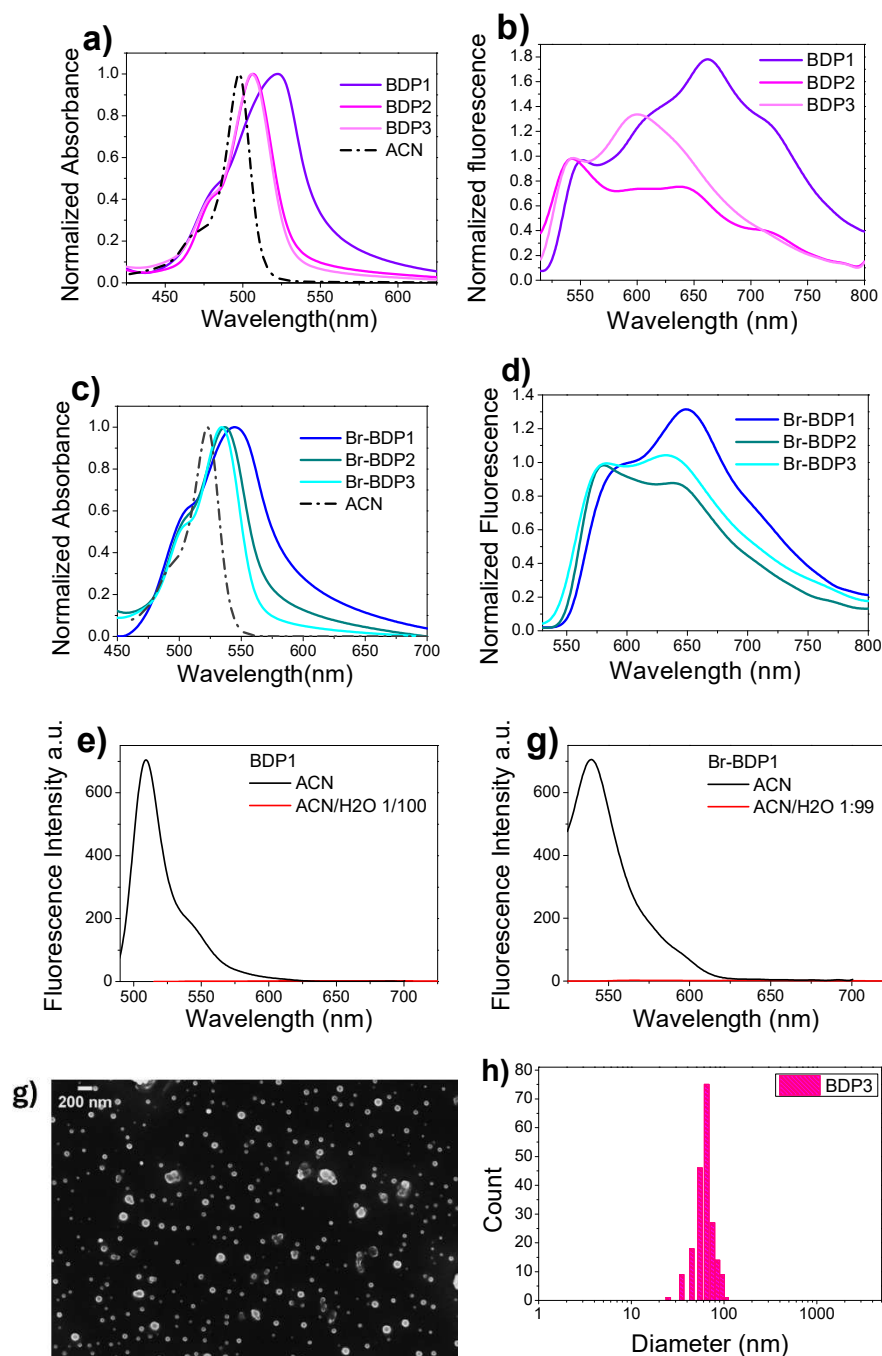


Figure 3: Absorption and fluorescence spectra of non-brominated a), b) and brominated c), d) compounds in a 1:99 ACN:water solution. Panels e) and f) compare the fluorescence intensity measured in pure ACN and 1:99 ACN:water mixture for compounds **BDP1** and **Br-BDP1**. Fluorescence has been recorded from solutions with matching absorbance. Panel g) and h) respectively report the SEM image and the size distribution analysis obtained for sample **BDP3**.

Concomitantly to changes in the absorption spectra, the emission of all samples drastically drops upon water addition, as shown in Figure 3e) and 3f) for representative non-brominated and brominated molecules (spectra of the remaining compounds are reported in Figure S2). The low intensity residual fluorescence band of the samples appears very broad and red-shifted as compared to the emission of the respective monomers (Figure 3b) and 3d)). The notable emission quenching suggests that in water the excited state of the samples relaxes mostly through non-radiative channels, possibly involving internal conversion and ISC. For aggregates, the intensity ratio between the main absorption peak and the blue-shifted vibronic shoulder decreases, passing from about 1:4 to 1:2 for all molecules. This observation, together with fluorescence quenching and the observed red-shift and broadening of the absorption band, leads to classification of the aggregates in terms of red-shifted H-aggregates.^[22]

To deeply ascertain the formation of aggregates and determine their morphology, SEM images were acquired, starting from the compounds dissolved in a 1:99 ACN:water mixed solvent. Images recorded for **BDP3** are reported in Figure 3g) as an example, data for the remaining compounds can be found in SI (Figure S9-S10). In all cases aggregates with spherical morphology were identified, whose average dimensions slightly depended on the specific molecule. The hydrodynamic radius as determined by DLS ranges from 130 nm to 220 nm (Table S3). The aggregates turned out to be very stable and could be observed with SEM also if starting from solutions stored in the dark for almost three months, without showing notable modification in their dimension and shape (see Figure S11).

2.3. Transient absorption spectroscopy

The photoinduced excited state dynamics of the samples have been investigated applying ultrafast pump-probe spectroscopy in the visible spectral range. Measurements were performed both in pure acetonitrile, to reveal the monomer behavior and in mixed ACN:water solvent, probing the photodynamic behavior of the aggregates. The excitation pulse has been set at 480 nm for monomers and 500 nm for aggregates. Global analysis has been performed to retrieve the kinetic constants associated with the excited state relaxation of the samples (SI section 1.2). In the case of all samples, we used a linear kinetic scheme, according to which each excited state evolves in a following intermediate state at lower energy, until complete excited state relaxation. Figure 4 reports the transient absorption data and the Evolution Associated Difference Spectra (EADS) obtained from global analysis for the monomers from **BDP1** and **BDP3** dissolved in ACN. The data from **BDP2** are reported in SI (Figure S3), but both the

transient spectra and the observed excited state dynamics are very similar to those described in case of **BDP3**.

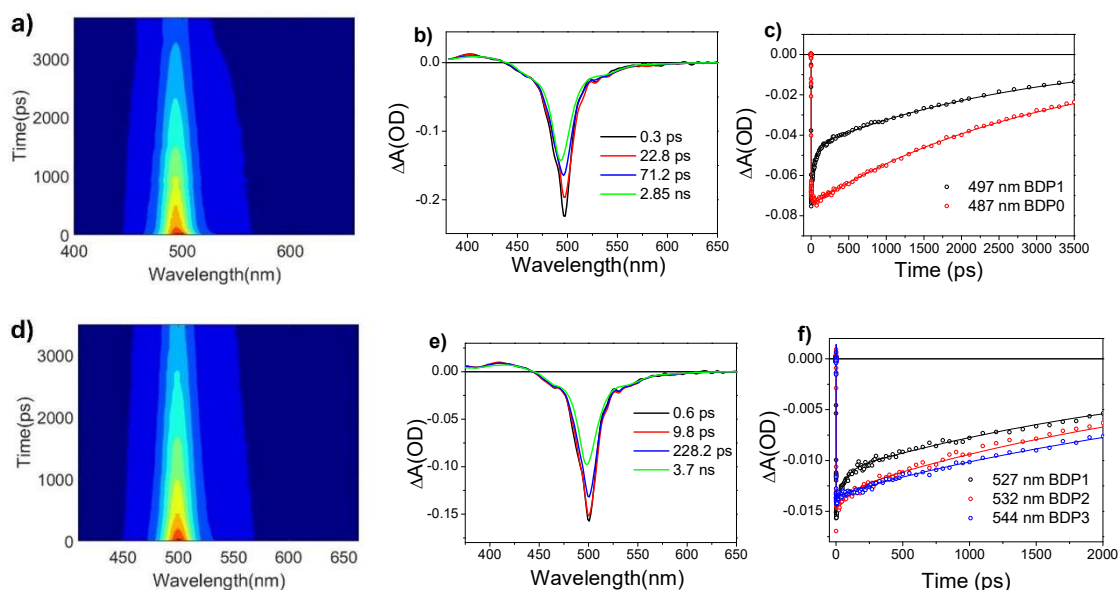


Figure 4: Transient absorption spectra of **BDP1** a) and **BDP3** d) recorded in ACN upon excitation at 480 nm. Panels b) and e) report the respective EADS obtained from global analysis of the recorded kinetic traces. Panel c) compares the kinetic trace at the maximum of the bleaching band for **BDP1** and the reference compound **BDP0**, while panel f) compares selected kinetic traces for **BDP1**, **BDP2**, and **BDP3**.

The transient spectra of both **BDP1** and **BDP3** present an intense negative band peaking at about 500 nm, assigned as ground state bleaching (GSB), which overlaps with the expected stimulated emission band (SE), because of the small Stokes shift, and a positive excited state absorption band (ESA), peaking at about 425 nm. For **BDP1** the signal recorded soon after excitation rapidly evolves in about 300 fs, showing a small intensity decrease of the GSB/SE band. Such rapid evolution signals a fast relaxation of the excited state, which evolves from the initially excited Frank Condon state because of electronic rearrangement and a fast inertial solvent response. The GSB intensity further decreases and slightly broadens within 22 ps. The evolution observed on this timescale is mostly associated with vibrational and solvent-induced relaxation. Within the following evolution, occurring in 74 ps, the maximum of the bleaching band apparently blue shifts by a few nm, while the intensity of the signal still decreases further. A small spectral change is also observed for the ESA band, whose intensity decreases around 400 nm, while it remains constant around 410 nm (see Figure S3 for details). We attribute this evolution to the occurrence of charge redistribution inside the molecule, with partial charge

transfer from the bodipy core towards the crown ether oxygens. This assignment is based on the identification of the spectral changes following bodipy oxidation through previous transient absorption studies, which results in the development of a positive band on the red side of the GSB signal and an evolution of the ESA band.^[23] Since there is not a complete electron transfer, but only a partial charge transfer for **BDP1**, spectral changes are quite limited. Nevertheless, the occurrence of charge redistribution has a notable effect on the excited state dynamics, as noticed by comparing the kinetic traces recorded for **BDP1** and **BDP0**, which lacks the appendant crown ether, as shown in Figure 4c). The excited state evolution of **BDP2** and **BDP3** is quite similar to that of **BDP1**. The difference is that for those two molecules, presenting positive charged groups inside the crown ether, the extent of charge redistribution between the bodipy core and the appendant is less than what observed for **BDP1**. As a consequence, the excited state lifetime results slightly longer, as noticed from the comparison of the GSB kinetic traces reported in Figure 3f. This is also in line with the increase of fluorescence QY for **BDP2** and **BDP3** as compared with **BDP1**, see Table 1.

The excited state evolution of the brominated molecules in ACN can be interpreted in a similar way, however for these compounds there is an additional excited state decay channel, due to the possibility of ISC.

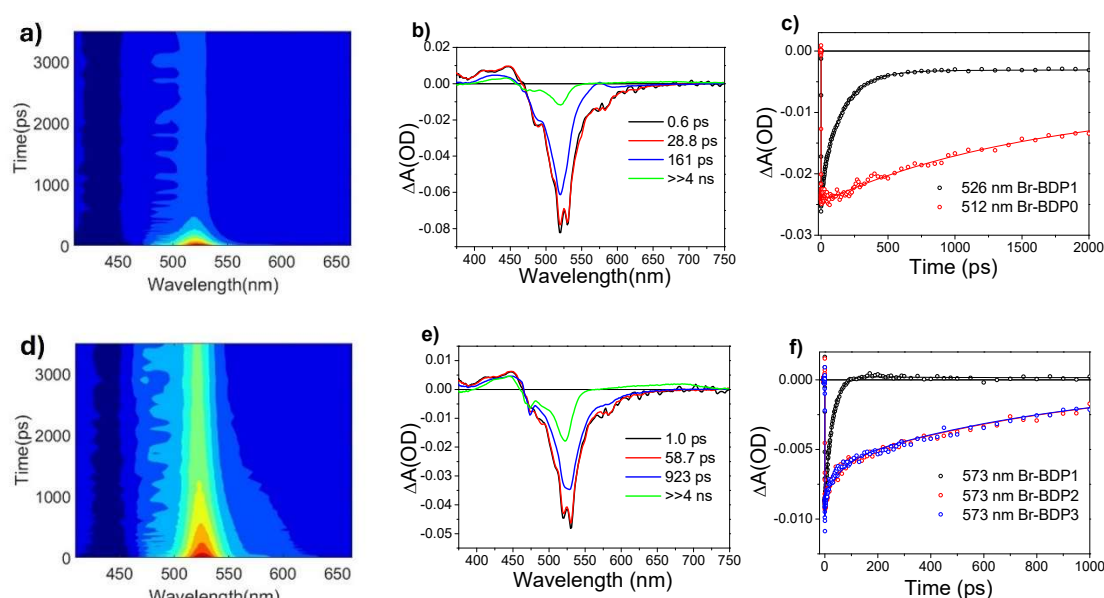


Figure 5: Transient absorption spectra of **Br-BDP1** a) and **Br-BDP3** d) recorded in ACN upon excitation at 480 nm. Panels b) and e) report the respective EADS obtained from global analysis of the recorded kinetic traces. Panel c) compares the kinetic trace at the maximum of the

bleaching band for **Br-BDP1** and the reference compound **Br-BDP0**, while panel f) compares selected kinetic traces of **Br-BDP1**, **Br-BDP2** and **Br-BDP3**.

As noticed in Figure 5, the influence of charge transfer is particularly evident for **Br-BDP1**. Indeed, the analysis of the EADS reported in Figure 5b) shows that a positive band at 575 nm rises within *ca* 28 ps, well noticed from the comparison with the kinetic traces with **Br-BDP0** in Figure 5c), indicating localization of positive charge on the bodipy core. The final spectral component retrieved for all the brominated molecules has the typical spectral shape of the bodipy triplet state, presenting a broad ESA which extends from about 525 nm to 750 nm.^[24] As it can be noticed from the transient spectra, the EADS and the kinetic traces reported in Figure 5 and Figure S4, also in the case of brominated compounds the extend of charge transfer reduces for compounds **Br-BDP2** and **Br-BDP3**, presenting charged groups inside the crown ether. This translates into increased fluorescence and triplet QY for those two samples as compared with **Br-BDP1**.

We then investigated the photodynamics of the aggregates, measuring the transient absorption spectra of all the compounds for different ACN:water ratios. Quite surprisingly the transient absorption spectra and the kinetic behavior of the compounds were all very similar, independently of the presence of bromine and only slightly dependent on the amount of added water, for ACN:water ratio $\geq 1:10$ (see Figure S5-S8). For all the aggregates the excited state lifetime is substantially shortened as compared to the respective monomers, indicating very efficient radiationless decay, also observed for aggregates formed when dissolving the samples in a 1:10 ACN:water mixed solvent (see Figure S5-S8). The analysis of the transient spectra of **BDP3** and **Br-BDP3**, reported in Figure 6 for aggregates obtained in a mixed 1:99 ACN:water solution, demonstrates that the photodynamics of both brominated and non-brominated samples can be described in the same way.

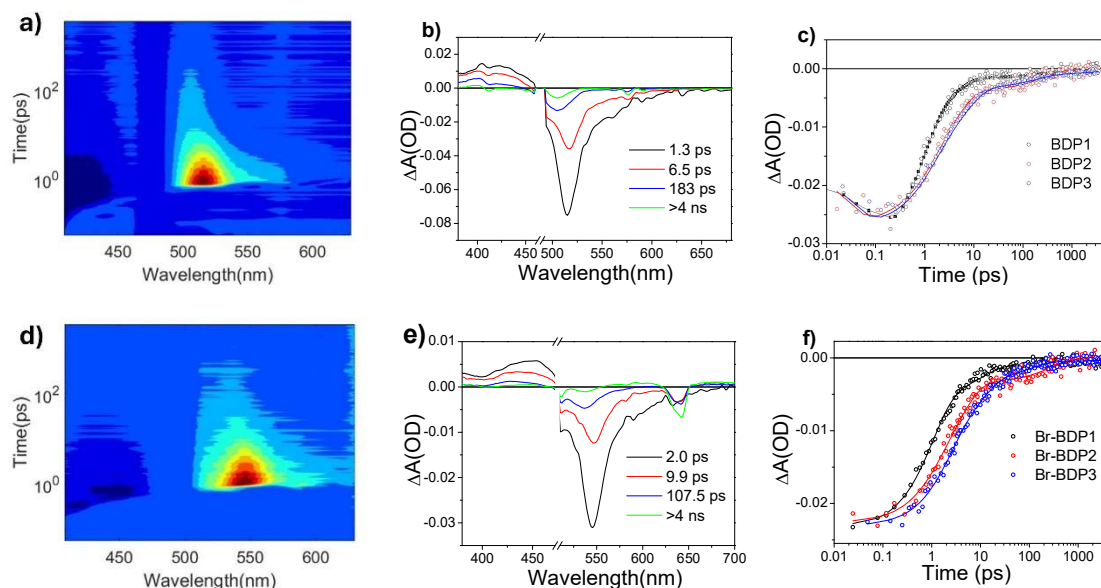


Figure 6: Transient absorption spectra of **BDP3** a) and **Br-BDP3** d) recorded in 1:99 ACN:water upon excitation at 500 nm. Panels b) and e) report the respective EADS obtained from global analysis of the recorded kinetic traces. Panel c) compares the kinetic trace at the maximum of the bleaching band for **BDP1**, **BDP2** and **BDP3** while panel f) compares the kinetic traces of the bleaching signal for **Br-BDP1**, **Br-BDP2** and **Br-BDP3**.

Soon after excitation, the transient spectra of both compounds present an intense negative band, peaking at the wavelength corresponding to the respective ground state absorption (514 nm for **BDP3** and 545 nm for **Br-BDP3**) and thus assigned as GSB, with a broad tail on its red side, ascribed to stimulated emission (SE). Furthermore, a positive ESA is observed, peaking at 420 nm for **BDP3** and 450 nm for **Br-BDP3**. The intensity of the signal substantially recovers within 2 ps for both samples, indicating a fast relaxation of the state initially reached upon photoexcitation, possibly assisted by solvation. On the following <10 ps timescale (6.5 ps for **BDP3** and 9.9 ps for **Br-BDP3**) we notice a further decay of the overall intensity of the transient signal and a blue-shift of the main negative peak, resulting from the almost complete recovery of the red-shifted SE. On the same timescale, the ESA band also changes its shape, decreasing in intensity and blue shifting. Considering what has already been observed for the monomers in a polar organic solvent, we attribute this evolution to the relaxation towards a CT state, most probably delocalized within the aggregate, possibly aided by vibrational relaxation. The relaxation towards a delocalized CT state has been recently reported for different aggregates, in particular for those formed by a heavy atom free photosensitizers based on cyanine chromophores.^[25] This delocalized CT state relaxes very quickly in the polar water environment, leading to the almost complete recovery of the transient signal within <200 ps. Such behavior

is consistently observed for all the compounds, with minor kinetic differences both between brominated and non-brominated molecules and between the systems with the empty crown ether and those presenting positively charged species inside the ether ring. Indeed, only a slightly faster recovery is observed in the case of **BDP1** and **Br-BDP1** if compared to the other aggregates, as shown in Figure 6c) and 6f). Notably, considering the extremely fast recovery of the excited state, the ISC channel appears suppressed, also in the presence of bromine, making the photodynamics of the aggregates independent from the presence of the heavy atom.

2.4 Photothermal properties

Although some of our compounds were initially engineered to efficiently form triplet states, the results presented above suggest that if dissolved in water, all the bodipy-crown ether adducts undergo very fast excited state relaxation, mostly through non-radiative pathways, also when Br atoms are introduced in the molecules. We thus evaluated the photothermal properties of the aggregates obtained in water, in view of their possible applications as photothermal antimicrobial agents. Indeed, numerous reported supramolecular assemblies display photothermal efficiencies rather high as compared to the respective monomers, providing a way to generate new and highly efficient photothermal materials, whose performances can be finely tuned by modulating the self-assembly conditions.^[26]

To evaluate their photothermal efficiency, the samples were irradiated with the 514 nm radiation produced by an Argon laser for about 10 minutes. The thermal changes were measured using a thermal camera (Figure 7). Irradiation was maintained until the temperature reached a plateau, then the laser was switched off to allow the solution gradually cool back to room temperature. Irradiation cycles were repeated three times for each sample to confirm the reversibility of the process and evaluate the stability of the systems. The photothermal efficiency (η) was evaluated according to the formula derived in reference.^[27] Details about the measurements can be found in SI, section 13. All the tested aggregates resulted in extremely efficient photothermal agents, with η values ranging between 70-99% (Supporting Information, Table S4).

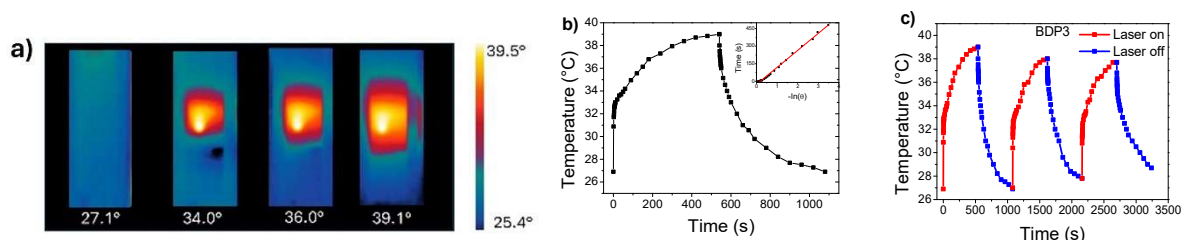


Figure 7: a) Thermal images recorded at different times for sample **BDP3** upon irradiation with an Ar laser (3 W/cm^2). The sample has been dissolved in a 1:99 ACN/water solvent at $100 \mu\text{M}$ concentration. b) Temperature rise of the solution during continuous irradiation for 500 s: after reaching a maximum temperature of about 40°C the laser has been switched off and the sample has been allowed to thermalize at room temperature. The inset of panel b) reports the linear temperature vs time data allowing to determine the constant for the heat transfer of the system, resulting 145.3 s for this sample. Panel c) reports three different heating cycles, confirming the reversibility of the process and showing only minimal degradation of the sample during heating.

2.5 Antimicrobial activity

The antibacterial activity of rotaxane-based bodipy PSs was investigated towards two bacterial strains, one Gram-positive strain (*Staphylococcus aureus* CIP76.25) and one Gram-negative strain (*Escherichia coli* CIP53.126). The Minimum Inhibitory Concentrations (MIC) and Minimum Bactericidal Concentrations (MBC) were determined. While MIC assays determine the lowest concentration of compounds preventing visible growth of a microorganism, MBC assays determine the lowest concentration reducing the viability of the initial bacterial inoculum by $\geq 99.9\%$ which represents a 3-log reduction of viability. Each experiment was realized in triplicate and repeated three times. The values of the MIC and MBC were measured in dark condition and after irradiation at 527 nm (with Green LED light, 69 mW.cm^{-2}) or with White LED light (78 mW.cm^{-2}) at a fluence of 25 J.cm^{-2} for each type of LED light

Table 2. Minimum Inhibitory Concentrations (MIC) determined for **BDP1-3** and **Br-BDP1-3** towards two bacterial strains under green or white light irradiation. **Br-BDP0** has also been tested as a control. All experiments were performed in triplicate. All MIC values except those indicated with an asterisk resulted consistently the same in the three repeated tests. The marked values are the average of the three measurements, further details are reported in SI, section 14.

Compound	MIC (μM)					
	<i>S. aureus</i> (CIP76.25)			<i>E. coli</i> (CIP53.126)		
	Green Light	White light	Dark	Green Light	White light	Dark
Br-BDP0	25	25	>200	>200	>200	>200
BDP1	> 200	> 200	> 200	> 200	> 200	> 200
Br-BDP1	> 200	> 200	> 200	> 200	> 200	> 200
BDP2	6.25	6.25	6.25	10.4*	12.5	6.25
Br-BDP2	6.25	6.25	3.125	50	25	6.25
BDP3	50	50	116.7*	> 200	50	> 200
Br-BDP3	4.17*	50	12.5	25	12.5	> 200

Table 3. Minimum Bactericidal Concentrations (MBC) determined for **BDP1-3** and **Br-BDP1-3** towards two bacterial strains under green or white light irradiation. **Br-BDP0** has also been tested as a control. All experiments were performed in triplicate. All MBC values resulted consistently the same in the three repeated tests.

Compound	MBC (μM)					
	<i>S. aureus</i> (CIP76.25)			<i>E. coli</i> (CIP53.126)		
	Green Light	White light	Dark	Green Light	White light	Dark
Br-BDP0	100	100	>200	>200	>200	>200
BDP1	> 200	> 200	> 200	> 200	> 200	> 200
Br-BDP1	> 200	> 200	> 200	> 200	> 200	> 200
BDP2	12.5	6.25	12.5	12.5	12.5	12.5
Br-BDP2	6.25	6.25	3.125	50	25	6.25
BDP3	100	50	> 200	> 200	50	> 200
Br-BDP3	6.25	50	12.5	25	12.5	> 200

The results showed that **BDP1** and **Br-BDP1** do not exhibit any cytotoxic activity regardless of the bacterial strain used both in the dark and after irradiation, since the MIC and MBC values exceeded 200 μM . This indicates that neither **BDP1** nor **Br-BDP1** are effective against these two bacterial strains under these specific conditions, indicating that the presence of the phosphonium-based axle is crucial to get antibacterial activities. **Br-BDP0** exhibits slightly higher cytotoxic activity against *S. aureus* compared to **Br-BDP1**, whereas *E. coli* remained insensitive to **Br-BDP0** under all illumination conditions.

Against *S. aureus*, **BDP2** and **Br-BDP2** exhibited a consistent MIC of 6.25 μM across all lighting conditions, indicating moderate and stable antibacterial activity under Green LED light, White LED light, and dark conditions. Their MIC and MBC values are relatively close, suggesting that **BDP2** and **Br-BDP2** are bactericidal. **BDP2** and **Br-BDP2** are less effective against *E. coli* than *S. aureus*. Surprisingly, **Br-BDP2** is more effective in dark conditions than after light irradiation. This cytotoxic activity could be due to the presence of phosphonium groups. A lower activity, after irradiation, could be explained by low photostability. Against *S. aureus*, **BDP3** showed photocytotoxic activity. Indeed, the MIC and MBC values are lower after irradiation than without light exposure. **Br-BDP3** demonstrated strong activity under Green LED light (4.17 μM) but showed reduced effectiveness in White LED light (50 μM). This indicates a light-dependent activity. The most interesting results are those observed against *E. coli*. In this case, **BDP3** showed a varied activity, with a MIC of 50 μM under White LED light but no significant effect (MIC > 200 μM) under Green LED light or in the dark, which is not surprising, considering the low absorbance of this compound at 527 nm. Inversely, **Br-BDP3** showed an interesting activity after light irradiation, both using the green LED, which well matches its absorption profile and under White light irradiation.

Comparing the various systems, we noticed that the presence of methoxy groups influences the activity of the compounds. Indeed, under dark conditions, **(Br)-BDP3** did not exhibit any antibacterial activity against *E. Coli*, while **(Br)-BDP2** showed bactericidal effects. A similar, though less pronounced, trend was observed with *S. aureus*. This result could be attributed to the influence of the electron-donating methoxy groups which disperse the positive charge on the phosphonium stoppers, thereby affecting the antibacterial activity.^[28]

In conclusion, **Br-BDP3** and **Br-BDP2** demonstrate potential as antibacterial agents, with **Br-BDP3** showing a strong response under green light and **Br-BDP2** performing well, especially

in the absence of light. Interestingly **BDP3**, not containing halogen atoms, demonstrates some light-induced antibacterial activity.

3. Conclusion

In this work we successfully synthesized and characterized novel photosensitizers for light-induced antimicrobial therapy based on the functionalization of bodipy dyes with triarylphosphonium rotaxanes. Three of our compounds, bearing two bromine atoms appended to the bodipy core, demonstrate efficient intersystem crossing as proven through transient absorption spectroscopy and can efficiently produce singlet oxygen upon photoexcitation in organic solvents. If dissolved in water, all the studied compounds self-assemble forming spherical nanoparticles, with narrow dimensional distribution and good stability, as shown by SEM microscopy and DLS analysis. Transient absorption spectroscopy demonstrates that the excited state lifetimes of all nanoparticles, independently of the presence of bromine, is highly reduced as compared with the respective monomers and intersystem crossing is mostly suppressed, also when halogen atoms are present in the structure. Considering that once excited the nanoparticles principally relax by internal conversion, thus releasing heat in their surroundings, we tested their efficiency as photothermal agents, by determining their photothermal conversion efficiency in water upon green light excitation. All the aggregates provided high photothermal conversion efficiency, with values reaching 90% in some cases. Finally, we conducted microbiological assays using two different bacterial strains to test the efficacy of the nanoparticles in antimicrobial light driven therapy. The obtained results indicate that both **Br-BDP3** and **Br-BDP2** have antibacterial capability, but while **Br-BDP3** is quite effective under green light illumination, **Br-BDP2** appears cytotoxic also in the absence of light. Finally, we noticed that **BDP3**, which doesn't contain halogen atoms, also demonstrates some light induced antibacterial activity.

Our results provide new insights into the application of bodipy based compounds in photomedicine. The possibility of exploiting self-assembly to produce effective nanoparticles not containing any halogen or heavy metal opens the way towards the development of biocompatible materials with high antibacterial efficiency.

Experimental Section/Methods

Details on the experimental methods can be found in Supporting Information

Supporting Information

Supporting Information is available from the Wiley Online Library or from the author.

Acknowledgements

M.D.D. acknowledges support from the European Union's Next Generation EU Program with the I-PHOQS Infrastructure [Nos. IR0000016, ID D2B8D520, and CUP B53C22001750006] “Integrated infrastructure initiative in Photonic and Quantum Sciences.”

C. C. thanks Nantes Université for a Ph.D. grant. C.C. and V.C. also thank CNRS for financial support. The authors greatly acknowledge AMaCC platform team (CEISAM UMR CNRS 6230, Nantes Université) for their contribution in mass spectrometry to this work. This work includes NMR experiments carried out on the CEISAM NMR platform. M.D.D. and G.S. thanks Dr Sara Nocentini for assistance regarding the photothermal measurements and Author 1 and Author 2 contributed equally to this work.

Received: ((will be filled in by the editorial staff))

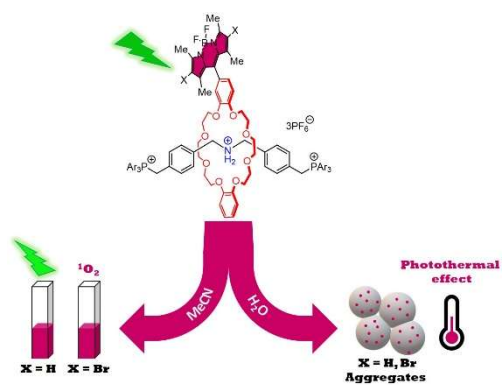
Revised: ((will be filled in by the editorial staff))

Published online: ((will be filled in by the editorial staff))

Table of contents entry

New photosensitizers for light induced antimicrobial therapy are successfully synthesized and characterized. When dissolved in water, all compounds self-assemble forming spherical aggregates with <100 nm dimensions. The nanoparticles show high photothermal conversion efficiency and demonstrate antimicrobial activity towards both Gram-negative and Gram-positive bacterial strains.

ToC figure



References

- [1] a)M. Frieri, K. Kumar, A. Boutin, Antibiotic resistance. *Journal of Infection and Public Health* **2017**, 10, 369; b)S. Hernando-Amado, T. M. Coque, F. Baquero, J. L. Martínez, Defining and combating antibiotic resistance from One Health and Global Health perspectives. *Nature Microbiology* **2019**, 4, 1432; c)A. MacGowan, E. Macnaughton, Antibiotic resistance. *Medicine* **2017**, 45, 622; d)E. Tacconelli, M. D. Pezzani, Public health burden of antimicrobial resistance in Europe. *The Lancet Infectious Diseases* **2019**, 19, 4.
- [2] a)L. S. Tzouvelekis, A. Markogiannakis, M. Psychogiou, P. T. Tassios, G. L. Daikos, Carbapenemases in *Klebsiella pneumoniae* and Other Enterobacteriaceae: an Evolving Crisis of Global Dimensions. *Clinical Microbiology Reviews* **2012**, 25, 682; b)A. Potron, L. Poirel, P. Nordmann, Emerging broad-spectrum resistance in *Pseudomonas aeruginosa* and *Acinetobacter baumannii*: Mechanisms and epidemiology. *International Journal of Antimicrobial Agents* **2015**, 45, 568; c)A. Carattoli, Plasmids and the spread of resistance. *International Journal of Medical Microbiology* **2013**, 303, 298.
- [3] C. A. Michael, D. Dominey-Howes, M. Labbate, The Antimicrobial Resistance Crisis: Causes, Consequences, and Management. *Frontiers in Public Health* **2014**, 2, 145.
- [4] a)C. P. Sabino, M. S. Ribeiro, M. Wainwright, C. dos Anjos, F. P. Sellera, M. Dropa, N. B. Nunes, G. T. P. Brancini, G. U. L. Braga, V. E. Arana-Chavez, R. O. Freitas, N. Lincopan, M. S. Baptista, The Biochemical Mechanisms of Antimicrobial Photodynamic Therapy. *Photochemistry and Photobiology* **2023**, 99, 742; b)H. Mahmoudi, A. Bahador, M. Pourhajibagher, M. Y. Alikhani, Antimicrobial Photodynamic Therapy: An Effective Alternative Approach to Control Bacterial Infections. *Journal of Lasers in Medical Sciences* **2018**, 9, 154; c)M. Piksa, C. Lian, I. C. Samuel, K. J. Pawlik, I. D. W. Samuel, K. Matczyszyn, The role of the light source in antimicrobial photodynamic therapy. *Chemical Society Reviews* **2023**, 52, 1697.
- [5] a)D. E. J. G. J. Dolmans, D. Fukumura, R. K. Jain, Photodynamic therapy for cancer. *Nature Reviews Cancer* **2003**, 3, 380; b)S. Ancély Ferreira dos, A. Daria Raquel Queiroz de, T. Leticia Ferreira, S. B. Maurício, L. Leticia, Photodynamic therapy in cancer treatment - an update review. *Journal of Cancer Metastasis and Treatment* **2019**, 5, 25; c)J. Choi, I.-C. Sun, H. Sook Hwang, H. Yeol Yoon, K. Kim, Light-triggered photodynamic nanomedicines for overcoming localized therapeutic efficacy in cancer treatment. *Advanced Drug Delivery Reviews* **2022**, 186, 114344.
- [6] a)T. Dai, Y.-Y. Huang, M. R. Hamblin, Photodynamic therapy for localized infections—State of the art. *Photodiagnosis and Photodynamic Therapy* **2009**, 6, 170; b)M. Tim, Strategies to optimize photosensitizers for photodynamic inactivation of bacteria. *Journal of Photochemistry and Photobiology B: Biology* **2015**, 150, 2; c)K. Sueoka, T. Chikama, Y. D. Pertiwi, J.-A. Ko, Y. Kiuchi, T. Sakaguchi, A. Obana, Antifungal efficacy of photodynamic therapy with TONS 504 for pathogenic filamentous fungi. *Lasers in Medical Science* **2019**, 34, 743.
- [7] K. Wang, B. Yu, J. L. Pathak, An update in clinical utilization of photodynamic therapy for lung cancer. *Journal of Cancer* **2021**, 12, 1154.
- [8] a)X. Wu, M. Yang, J. S. Kim, R. Wang, G. Kim, J. Ha, H. Kim, Y. Cho, K. T. Nam, J. Yoon, Reactivity Differences Enable ROS for Selective Ablation of Bacteria. *Angewandte Chemie International Edition* **2022**, 61, e202200808; b)H. Kim, Y. R. Lee, H. Jeong, J. Lee, X. Wu, H. Li, J. Yoon, Photodynamic and photothermal therapies for bacterial infection treatment. *Smart Molecules* **2023**, 1, e20220010; c)X. Yuan, S. Suárez-García, M. De Corato, A. C. Muñoz, I. Pagonabarraga, D. Ruiz-Molina, K. Villa, Self-Degradable Photoactive Micromotors for Inactivation of Resistant Bacteria. *Advanced Optical Materials* **2024**, 12, 2303137.

- [9] a)H. Lu, J. Mack, Y. Yang, Z. Shen, Structural modification strategies for the rational design of red/NIR region BODIPYs. *Chemical Society Reviews* **2014**, 43, 4778; b)J. Wang, Q. Gong, L. Wang, E. Hao, L. Jiao, The main strategies for tuning BODIPY fluorophores into photosensitizers. *Journal of Porphyrins and Phthalocyanines* **2020**, 24, 603.
- [10] N. Boens, B. Verbelen, M. J. Ortiz, L. Jiao, W. Dehaen, Synthesis of BODIPY dyes through postfunctionalization of the boron dipyrromethene core. *Coordination Chemistry Reviews* **2019**, 399, 213024.
- [11] S. J. Rowan, S. J. Cantrill, J. F. Stoddart, Triphenylphosphonium-Stoppered [2]Rotaxanes. *Organic Letters* **1999**, 1, 129.
- [12] Y. Ohishi, T. Ichikawa, S. Yokoyama, J. Yamashita, M. Iwamura, K. Nozaki, Y. Zhou, J. Chiba, M. Inouye, Water-Soluble Rotaxane-Type Porphyrin Dyes as a Highly Membrane-Permeable and Durable Photosensitizer Suitable for Photodynamic Therapy. *ACS Applied Bio Materials* **2024**, 7, 6656.
- [13] a)T. Sprenger, T. Schwarze, H. Müller, E. Sperlich, A. Kelling, H.-J. Holdt, J. Paul, V. Martos Riaño, M. Nazaré, BODIPY-Equipped Benzo-Crown-Ethers as Fluorescent Sensors for pH Independent Detection of Sodium and Potassium Ions. *ChemPhotoChem* **2023**, 7, e202200270; b)T. Sprenger, T. Schwarze, H.-J. Holdt, A. Hentsch, M. Nazaré, Benzo-Crown-Ether Functionalized O-BODIPY Probes for Cations – A Selective Fluorescent Probe for Ba²⁺. *Chemistry – A European Journal* **2024**, 30, e202401928.
- [14] E. Bassan, A. Gualandi, P. G. Cozzi, P. Ceroni, Design of BODIPY dyes as triplet photosensitizers: electronic properties tailored for solar energy conversion, photoredox catalysis and photodynamic therapy. *Chemical Science* **2021**, 12, 6607.
- [15] a)J. Yao, H. Li, Y.-N. Xu, Q.-C. Wang, D.-H. Qu, Efficient Intramolecular Energy Transfer between Two Fluorophores in a Bis-Branched [3]Rotaxane. *Chemistry – An Asian Journal* **2014**, 9, 3482; b)R. Arumugaperumal, V. Srinivasadesikan, M. V. Ramakrishnam Raju, M.-C. Lin, T. Shukla, R. Singh, H.-C. Lin, Multi-stimuli-responsive high contrast fluorescence molecular controls with a far-red emitting BODIPY-based [2]rotaxane. *ACS Applied Materials & Interfaces* **2015**, 7, 26491; c)R. Arumugaperumal, P. Venkatesan, T. Shukla, P. Raghunath, R. Singh, S.-P. Wu, M.-C. Lin, H.-C. Lin, Acid/Base and H₂PO₄–Controllable High-Contrast Optical Molecular Switches with a Novel BODIPY Functionalized [2]Rotaxane. *Sensors and Actuators B: Chemical* **2018**, 270, 382; d)N. Yesilgul, O. Seven, R. Guliyev, E. U. Akkaya, Energy Harvesting in a Bodipy-Functionalized Rotaxane. *The Journal of Organic Chemistry* **2018**, 83, 13228; e)S.-M. Chan, F.-K. Tang, C.-S. Kwan, C.-Y. Lam, S. C. K. Hau, K. C.-F. Leung, Water-compatible fluorescent [2]rotaxanes for Au³⁺ detection and bioimaging. *Materials Chemistry Frontiers* **2019**, 3, 2388.
- [16] J. Sun, W. Li, Y. Hou, X. Zhang, Z. Gao, B. Wang, J. Zhao, a-PET and Weakened Triplet–Triplet Annihilation Self-Quenching Effects in Benzo-21-Crown-7-Functionalized Diiodo-BODIPY. *ACS Omega* **2021**, 6, 28356.
- [17] M. Grimmeisen, C. Jessen-Trefzer, Increasing the Selectivity of Light-Active Antimicrobial Agents – Or How To Get a Photosensitizer to the Desired Target. *ChemBioChem* **2023**, 24, e202300177.
- [18] H.-B. Cheng, X. Cao, S. Zhang, K. Zhang, Y. Cheng, J. Wang, J. Zhao, L. Zhou, X.-J. Liang, J. Yoon, BODIPY as a Multifunctional Theranostic Reagent in Biomedicine: Self-Assembly, Properties, and Applications. *Advanced Materials* **2023**, 35, 2207546.
- [19] a)R. Bresolí-Obach, I. Gispert, D. G. Peña, S. Boga, Ó. Gulias, M. Agut, M. E. Vázquez, S. Nonell, Triphenylphosphonium cation: A valuable functional group for antimicrobial photodynamic therapy. *Journal of Biophotonics* **2018**, 11, e201800054; b)M. A. Masood, Y. Wu, Y. Chen, H. Yuan, N. Sher, F. Faiz, S. Yao, F. Qi, M. I. Khan, M. Ahmed, N. Mushtaq, W. He, Z. Guo, Optimizing the photodynamic therapeutic effect of BODIPY-based photosensitizers against cancer and bacterial cells. *Dyes and Pigments* **2022**, 202,

- 110255; c)I. Chaves, F. M. P. Morais, C. Vieira, M. Bartolomeu, M. A. F. Faustino, M. G. P. M. S. Neves, A. Almeida, N. M. M. Moura, Can Porphyrin–Triphenylphosphonium Conjugates Enhance the Photosensitizer Performance Toward Bacterial Strains? *ACS Applied Bio Materials* **2024**, 7, 5541.
- [20] E. R. H. Walter, P. K.-K. Leung, L. C.-C. Lee, K. K.-W. Lo, N. J. Long, Potent BODIPY-based photosensitisers for selective mitochondrial dysfunction and effective photodynamic therapy. *Journal of Materials Chemistry B* **2024**.
- [21] a)Z. Chen, Z. Chen, Functional supramolecular aggregates based on BODIPY and aza-BODIPY dyes: control over the pathway complexity. *Organic Chemistry Frontiers* **2023**, 10, 2581; b)X. Miao, H. Tao, W. Hu, Y. Pan, Q. Fan, W. Huang, *Science China Chemistry* **2020**, 63, 1075; c)J. Miao, G. Yao, Y. Huo, B. Wang, W. Zhao, W. Guo, Constructing Heavy-Atom-Free Photosensitizers for Hypoxic Tumor Phototherapy Based on Donor-Excited Photoinduced Electron-Transfer-Driven Type-I and Type-II Mechanisms. *ACS Applied Materials & Interfaces* **2024**, 16, 40428; d)S. Ghosh, S. Mula, P. Biswas, A. Patra, Ultrafast Photoinduced Dynamics of Styryl-Substituted BODIPY Dyes and Their Aggregates. *The Journal of Physical Chemistry C* **2024**, 128, 12762; e)H. Wen, Q. Wu, C. Li, T. Sun, Z. Xie, 4,4-Difluoro-4-bora-3a,4a-diaza-s-indacene (BDPI)-Triphenylphosphine Nanoparticles as a Photodynamic Antibacterial Agent. *ACS Applied Nano Materials* **2022**, 5, 1500.
- [22] N. J. Hestand, F. C. Spano, Expanded Theory of H- and J-Molecular Aggregates: The Effects of Vibronic Coupling and Intermolecular Charge Transfer. *Chemical Reviews* **2018**, 118, 7069.
- [23] A. Iagatti, L. Cupellini, G. Biagiotti, S. Caprasecca, S. Fedeli, A. Lapini, E. Ussano, S. Cicchi, P. Foggi, M. Marcaccio, B. Mennucci, M. Di Donato, Efficient Photoinduced Charge Separation in a BODIPY–C60 Dyad. *The Journal of Physical Chemistry C* **2016**, 120, 16526.
- [24] a)K. Chen, W. Yang, Z. Wang, A. Iagatti, L. Bussotti, P. Foggi, W. Ji, J. Zhao, M. Di Donato, Triplet Excited State of BODIPY Accessed by Charge Recombination and Its Application in Triplet–Triplet Annihilation Upconversion. *The Journal of Physical Chemistry A* **2017**, 121, 7550; b)Y. Liu, J. Zhao, A. Iagatti, L. Bussotti, P. Foggi, E. Castellucci, M. Di Donato, K.-L. Han, A Revisit to the Orthogonal Bodipy Dimers: Experimental Evidence for the Symmetry Breaking Charge Transfer-Induced Intersystem Crossing. *The Journal of Physical Chemistry C* **2018**, 122, 2502; c)Z. Wang, A. Toffoletti, Y. Hou, J. Zhao, A. Barbon, B. Dick, Insight into the drastically different triplet lifetimes of BODIPY obtained by optical/magnetic spectroscopy and theoretical computations. *Chemical Science* **2021**, 12, 2829.
- [25] X. Zhao, S. He, J. Wang, J. Ding, S. Zong, G. Li, W. Sun, J. Du, J. Fan, X. Peng, Near-Infrared Self-Assembled Hydroxyl Radical Generator Based on Photoinduced Cascade Electron Transfer for Hypoxic Tumor Phototherapy. *Advanced Materials* **2023**, 35, 2305163.
- [26] L. Zhao, Y. Liu, R. Xing, X. Yan, Supramolecular Photothermal Effects: A Promising Mechanism for Efficient Thermal Conversion. *Angewandte Chemie International Edition* **2020**, 59, 3793.
- [27] D. K. Roper, W. Ahn, M. Hoepfner, Microscale Heat Transfer Transduced by Surface Plasmon Resonant Gold Nanoparticles. *The Journal of Physical Chemistry C* **2007**, 111, 3636.
- [28] C. D. Kodjo Amengor, C. Amaning Danquah, E. B. A. Adusei, F. K. Kekessie, F. Ofosu-Koranteng, P. Peprah, B. K. Harley, E. Orman, J. Adu, Y. Saaka, Synthesized Phosphonium Compounds Demonstrate Resistant Modulatory and Antibiofilm Formation Activities against Some Pathogenic Bacteria. *Heteroatom Chemistry* **2022**, 2022, 7411957.